

# D irac quasinorm al m odes of the R eissner-N ordstrom de Sitter black hole

Jiliang Jing

Institute of Physics and Department of Physics,

Hunan Normal University,

Changsha, Hunan 410081, P . R . China

and

School of Mathematics and Statistics,

University of Newcastle Upon Tyne,

Newcastle Upon Tyne NE1 7RU, UK

The quasinormal modes of the Reissner-Nordström de Sitter black hole for the massless Dirac fields are studied using the Post-Newtonian approximation. We find that the magnitude of the imaginary part of the quasinormal frequencies decreases as the cosmological constant or the orbital angular momentum increases, but it increases as the charge or the overtone number increases. An interesting feature is that the imaginary part is almost linearly related to the real part as the cosmological constant changes for fixed charge, and the linearity becomes better as the orbital angular momentum increases. We also prove exactly that the Dirac quasinormal frequencies are the same for opposite chirality.

PACS numbers: 04.70.-s, 04.50.+h, 11.15.-q, 11.25.Hf

## I. INTRODUCTION

It is well known that dynamical evolution of field perturbation on a black hole background can be roughly divided into three stages [1]. The first one is an initial wave burst coming directly from the source of perturbation and is dependent on the initial form of the original field perturbation. The second one involves the damped oscillations which frequencies and damping times are entirely fixed by the structure of the background spacetime and are independent of the initial perturbation. This stage can be accurately described in terms of the discrete set of quasinormal modes (QNM's). And the last one is a power-law tail behavior of the waves at very late time which is caused by backscattering of the gravitational field.

QNM's of a black hole are defined as proper solutions of the perturbation equations belonging to certain complex characteristic frequencies which satisfy the boundary conditions appropriate for purely ingoing waves at the event horizon and purely outgoing waves at infinity [2]. It is generally believed that QNM's carry a unique footprint to directly identify the black hole existence. Through the QNM's, one can extract information of the physical parameters of the black hole, mass, electric charge, and angular momentum, from the gravitational wave signal by fitting the few lowest observed quasinormal frequencies to those calculated from the perturbation analysis, as well as test the stability of the event horizon against small perturbations. Moreover, QNM's may be related to fundamental physics, such as the thermodynamic properties of black holes in loop quantum gravity [3] [4].

The idea of QNM's in asymptotically flat black hole started with the work of Vishveshwara [5], and the actually numerical calculation of the quasinormal frequencies was first presented by Chandrasekhar and Detweiler [2]. Since then great effort has been contributed to calculate QNM's of asymptotically flat black holes [6] [7]. QNM's in asymptotically flat spacetimes have recently acquired a further importance since the real part of the quasinormal frequencies with a large imaginary part is equal to the Barbero-Immirzi parameter [3] [4] [8] [9], a factor introduced by hand in order that loop quantum gravity reproduces correctly entropy of the black hole.

Recently a new application of the quasinormal mode spectrum has also arisen from superstring theory [10] [11] [12]. There is a suggestion, known as the AdS/CFT correspondence, that string theory in anti-de Sitter (AdS) space is equivalent to conformal field theory (CFT) in one less dimension [10] [11] [12]. According to the AdS/CFT correspondence, a large static black hole in asymptotically AdS spacetime corresponds to a thermal state in CFT, and the decay of the test field in the black hole spacetime corresponds to the decay of the perturbed state in CFT. Thus the quasinormal frequencies give us the thermalization time scale which is

very hard to compute directly. Therefore, many authors have delved into the studies of QNM s for different asymptotically AdS black holes [13, 14, 15, 16, 17, 18, 19, 20, 21, 22].

There is considerable observational evidence that the physical universe has a positive cosmological constant [23, 24, 25]. This observation is at least partially responsible for the recent flurry of investigations into asymptotically de Sitter spacetimes. In particular, the study of QNM s in asymptotically de Sitter spacetimes has garnered much attention [26, 27, 28, 29, 30, 31]. Moss and collaborators [26] first carried out the calculation of the quasinormal frequencies for the gravitational perturbations of the Schwarzschild de Sitter black hole. Cardoso and Lemos [27] devised an analytical method to study the case in which the black hole and the cosmological horizons are very close to each other. Molina [28] extended the analytical method to higher dimensional Schwarzschild de Sitter black holes, and Maaßen [29] used it to study the quasinormal mode spectrum of the Schwarzschild de Sitter black hole for the scalar, the electromagnetic, and the gravitational fields in the limit of nearly equal black hole and cosmological radii. Zhidenko [31] calculated the low-laying quasinormal frequencies of the Schwarzschild de Sitter black hole for fields of different spin by using the sixth-order WKB and the Post-Newtonian potential approximations. However, the question how the charge of a asymptotically de Sitter black hole affects the quasinormal frequencies still remains open. The main purpose of this paper is to study the question by calculating the Dirac quasinormal frequencies of the Reissner-Nordstrom de Sitter black hole.

The paper is organized as follows: In Sec. II, the massless Dirac field equation in the Reissner-Nordstrom de Sitter black hole spacetime is decoupled by introducing a tetrad. In Sec. III, the relation between the quasinormal modes spectra for the Dirac particles and the antiparticles is discussed. In Sec. IV, the quasinormal frequencies are calculated and the results are presented by tables and figures. The last section devotes to summary and discussions.

## II. DIRAC EQUATION IN REISSNER-NORDSTROM DE SITTER BLACK HOLE SPACETIME

In standard coordinates, the metric for the Reissner-Nordstrom de Sitter black hole can be expressed as

$$ds^2 = f dt^2 + \frac{1}{f} dr^2 + r^2 (d^2 + \sin^2 d'^2); \quad (2.1)$$

with

$$f = 1 - \frac{2M}{r} + \frac{Q^2}{r^2} - \frac{1}{3} r^2; \quad (2.2)$$

where the parameters  $M$ ,  $Q$ , and  $\Lambda$  represent the black hole mass, the charge, and the cosmological constant, respectively.

In order to separate the massless Dirac equation [32]

$$[\bar{e}_a (\partial_t + \omega)] = 0; \quad (2.3)$$

where  $\bar{e}$  is the Dirac matrix,  $e_a$  is the inverse of the tetrad  $e^a$ , and  $\omega$  is the spin connection which is defined as  $\omega = \frac{1}{8} [\bar{e}^a; \bar{e}^b] e_a e_b$ , we take the tetrad as

$$e^a = \text{diag}(\frac{P}{f}; \frac{1}{Pf}; r; r \sin\theta); \quad (2.4)$$

Then, the Dirac equation (2.3) becomes

$$\bar{e}^0 \frac{\partial}{\partial t} + \bar{e}^1 \frac{\partial}{\partial r} - \frac{\partial}{\partial r} + \frac{1}{r} + \frac{1}{4f} \frac{df}{dr} + \frac{2}{r} (\frac{\partial}{\partial r} + \frac{1}{2} \cot\theta) + \frac{3}{r \sin\theta} \frac{\partial}{\partial\theta} = 0; \quad (2.5)$$

If we define

$$= f^{-\frac{1}{4}}; \quad (2.6)$$

Eq. (2.5) can be simplified as

$$\bar{e}^0 \frac{\partial}{\partial t} + \bar{e}^1 \frac{\partial}{\partial r} - \frac{\partial}{\partial r} + \frac{1}{r} + \frac{2}{r} (\frac{\partial}{\partial r} + \frac{1}{2} \cot\theta) + \frac{3}{r \sin\theta} \frac{\partial}{\partial\theta} = 0; \quad (2.7)$$

Introducing a tortoise coordinate change

$$r^z = \frac{dr}{f}; \quad (2.8)$$

and the ansatz

$$= \frac{\frac{iG^{(+)}(r)}{F^{(+)}(r)}}{\frac{iG^{(-)}(r)}{F^{(-)}(r)}} e^{i!t}; \quad (2.9)$$

with

$${}_{jm}^+ = @ q \frac{0}{q} \frac{q}{\frac{j+m}{2j} Y_1^m} {}_{1=2}^1 A; \quad (\text{for } j = l + \frac{1}{2});$$

$${}_{jm}^- = @ q \frac{0}{q} \frac{q}{\frac{j+1-m}{2j+2} Y_1^m} {}_{1=2}^1 A; \quad (\text{for } j = l - \frac{1}{2});$$

we find that the cases for (+) and (-) in the functions F and G can be put together, and then the decoupled equations can be written as

$$\frac{d^2 F}{dr^2} + (!^2 V_1) F = 0; \quad (2.10)$$

$$\frac{d^2 G}{dr^2} + (!^2 V_2) G = 0; \quad (2.11)$$

with

$$V_1 = \frac{p \bar{f} \bar{k}^j}{r^2} \bar{k}^j \frac{p}{\bar{f}} + \frac{r df}{2 dr} f; \quad \text{for } k = j + \frac{1}{2}; \quad \text{and } j = l + \frac{1}{2}; \quad (2.12)$$

$$V_2 = \frac{p \bar{f} \bar{k}^j}{r^2} \bar{k}^j \frac{p}{\bar{f}} - \frac{r df}{2 dr} f; \quad \text{for } k = -j + \frac{1}{2}; \quad \text{and } j = l - \frac{1}{2}; \quad (2.13)$$

The potentials possess two special properties: a) They are related to the metric function  $\bar{f}$ , which complicate the calculation of the quasinormal frequencies. b) There is no quasinormal modes for  $l = 0$  for potential  $V_2$  because  $\bar{k}^j = j!$  in this case. If we set  $Q = 0$  and  $Q = 0$  the equations (2.10)–(2.13) give the results of the Schwarzschild black hole [33]. In the following we will use the equations (2.10)–(2.13) to study Dirac quasinormal frequencies.

### III. RELATION BETWEEN THE CHARACTERISTIC FREQUENCIES FOR DIRAC PARTICLES AND ANTIPARTICLES

In this section we shall prove that Dirac particles and antiparticles have the same quasinormal mode spectra in the Reissner-Nordstrom de Sitter black hole spacetime.

Introducing a function

$$W = \frac{\bar{k}^j \bar{f}}{r}; \quad (3.1)$$

the potentials (2.12) and (2.13) can be rewritten as

$$V_1 = \frac{dW}{dr} + W^2; \quad (3.2)$$

$$V_2 = -\frac{dW}{dr} + W^2; \quad (3.3)$$

which show that the two potentials are supersymmetric partners derived from the same superpotential  $W$ . Now we rewrite metric function (2.2) as

$$f = \frac{1}{3r^2} (r - r_-)(r - r_+)(r_c - r)(r - r_b); \quad (3.4)$$

where  $r_c$ ,  $r_+$ , and  $r_-$  represent the cosmological horizon, the outer event horizon, and the inner event horizon, respectively, and  $r_b$  can be determined by using  $r_c$ ,  $r_+$ , and  $r_-$ . Then the tortoise coordinate (2.8) can be expressed as

$$\begin{aligned} r &= \frac{z}{f} \\ &= \frac{1}{2} \left( \frac{1}{r-r_-} \ln(r-r_-) + \frac{1}{r-r_+} \ln(r-r_+) - \frac{1}{c} \ln(r_c-r) + \frac{1}{b} \ln(r-r_b) \right); \end{aligned} \quad (3.5)$$

where  $i = \frac{1}{2} \frac{df}{dr} \Big|_{r=r_+}$ . From Eq. (3.5) we find

$$\begin{aligned} r &\rightarrow 1 && \text{as } r \rightarrow r_+; \\ r &\rightarrow +1 && \text{as } r \rightarrow r_c; \end{aligned} \quad (3.6)$$

Therefore, it is obviously that  $W$  is an arbitrary smooth function over the range of  $r$ , ( $1; +1$ ). And the superpotential function, together with its derivatives of all orders with respect to  $r$ , vanish for both  $r \rightarrow 1$  and  $r \rightarrow +1$ . From above discussions we know that the potentials  $V_1$  and  $V_2$  also are smooth functions, integrable over the range of  $r$ , ( $1; +1$ ), and they vanish exponentially as we approach both the event horizon  $r_+$  and the cosmological horizon  $r_c$ , i.e.,

$$\begin{aligned} V_{1,2} &\rightarrow e^{2\phi(r)}; && \text{as } r \rightarrow 1 \\ V_{1,2} &\rightarrow e^{-2\phi(r)}; && \text{as } r \rightarrow +1; \end{aligned} \quad (3.7)$$

Eqs. (2.10), (2.11), and (3.7) show that the asymptotic behaviour of the solutions,  $F$  and  $G$ , for  $r \rightarrow 1$ , can be described by

$$e^{i\omega r}; \quad (r \rightarrow 1); \quad (3.8)$$

Ref. [34] pointed out that there is no restriction to supposing that, given a solution  $G$  of equation (2.11),

$$F = pG + q \frac{dG}{dr}; \quad (3.9)$$

is a solution of equation (2.10), where  $p$  and  $q$  are certain suitably chosen functions which satisfy the relations [34]

$$q(V_1 - V_2) = 2 \frac{dp}{dr} + \frac{d^2q}{dr^2}; \quad (3.10)$$

$$p^2 + p \frac{dq}{dr} - q \frac{dp}{dr} - q^2 (V_2 - \omega^2) = \text{const} = C^2; \quad (3.11)$$

For the potentials  $V_1$  and  $V_2$  we can verify that

$$q = 1; \quad p = W; \quad (3.12)$$

satisfy Eqs. (3.10) and (3.11) with  $C^2 = \omega^2$ . Accordingly, the solutions  $F$  and  $G$  of Eqs. (2.10) and (2.11) are related in the manner

$$i\omega F = W G + \frac{dG}{dr} = \frac{\frac{p}{r} \bar{f}}{r} G + \frac{dG}{dr}; \quad (3.13)$$

where we have chosen a relative normalization of  $F$  and  $G$  so that the inverse relation in the same normalization is

$$i\omega G = W F + \frac{dF}{dr} = \frac{\frac{p}{r} \bar{f}}{r} F + \frac{dF}{dr}; \quad (3.14)$$

The quasinormal modes are defined as solutions of Eqs. (2.10) and (2.11), belonging to complex characteristic frequencies and satisfying the boundary conditions

$$\begin{aligned} F &\rightarrow A^{(+)}(\omega) e^{-i\omega r}; && r \rightarrow +1; \\ &\rightarrow e^{+i\omega r}; && r \rightarrow +1; \\ G &\rightarrow A^{(-)}(\omega) e^{-i\omega r}; && r \rightarrow +1; \\ &\rightarrow e^{+i\omega r}; && r \rightarrow +1; \end{aligned} \quad (3.15)$$

If  $\omega$  is a characteristic frequency and  $G$  is the solution belonging to it, then the solution  $F$  derived from  $G$  by Eq. (3.13) will satisfy the boundary conditions (3.15) with

$$A^{(+)}(\omega) = e^{i\omega t} A^{(-)}(\omega); \quad (3.16)$$

Thus, the characteristic frequencies are the same for both  $F$  and  $G$ . Physically the result indicates that Dirac particles and antiparticles have the same quasinormal mode spectra in the Reissner-Nordstrom de Sitter black hole spacetime. We shall therefore concentrate just on Eq. (2.10) with potential  $V_1$  in evaluating the quasinormal frequencies in the next section.

#### IV. DIRAC QUASINORMAL FREQUENCIES IN THE REISSNER-NORDSTROM DE SITTER BLACK HOLE SPACETIME

Moss and Nomran [26] found that the gravitational QNMs of the Schwarzschild-de Sitter black hole calculated by the Leaver approach [35] agree with the results by using the Poshl-Teller potential approximation for low overtone, and Zhdanenko [31] showed that the quasinormal mode frequencies obtained by the Poshl-Teller approximation and the sixth-order WKB approximation are in a very good agreement for the Schwarzschild de Sitter black hole. The reason why the results obtained by the Poshl-Teller potential approximation are good agreement with other numerical results is that the potentials of black holes in de Sitter space fall off exponentially. Therefore, for the Reissner-Nordstrom de Sitter black hole we can study the Dirac quasinormal modes by using the Poshl-Teller approximate potential [36] [37] [38].

$$V_{PT} = \frac{V_0}{\cosh^2(r-b)}; \quad (4.1)$$

The potential contains two free parameters ( $V_0$  and  $b$ ) which are used to fit the height and the second derivative of the potential at the maximum. The location of the maximum has to be found numerically. From the potentials (2.12) and (2.13) we find that the position of the potential peak as  $|kj| = 1$  is

$$r_0(kj=1) = \frac{3}{2}M + \frac{3}{2}M - 1 - \frac{8Q^2}{9M^2}; \quad (4.2)$$

and

$$r_0(kj) = r_0(kj=1); \quad (\text{for } V1); \quad (4.3)$$

$$r_0(kj) = r_0(kj=1); \quad (\text{for } V2); \quad (4.4)$$

If we use the mass  $M$  of the black hole as a unit of mass and length, the value of the  $r_0(kj=1)$  just relies on the charge  $Q$ . It gives  $r_0(kj=1) = 3$  for an uncharged black hole, which agrees with result for the Schwarzschild-de Sitter black hole in Refs. [26] [33]. We should point out that although  $r_0(kj=1)$  does not depend on the cosmological constant,  $r_0(kj)$  does in general.

The quasinormal frequencies of the Poshl-Teller potential can be evaluated analytically [37] [38]

$$\omega_n = \frac{1}{b} \sqrt{\frac{V_0 b^2}{4} - \frac{1}{4}} \left( n + \frac{1}{2} \right)^{\frac{1}{2}} i; \quad (n = 0, 1, 2, \dots); \quad (4.5)$$

However, the quantities  $V_0$  and  $b$  for different  $Q$  and  $kj$  should be found numerically. The quasinormal frequencies of the Dirac particles in the Reissner-Nordstrom de Sitter black hole spacetime for different  $Q$ ,  $kj$  and  $n$  are presented in tables I-VIII and figures 1-6.

In the calculation we hold 85 digits in all intermediate values and use the black hole mass units.

#### V. SUMMARY AND DISCUSSIONS

The quasinormal mode frequencies of the Reissner-Nordstrom de Sitter black hole for the massless Dirac fields are studied by using Poshl-Teller potential approximation. The results indicate that the quasinormal frequencies are determined by the mass  $M$ , the charge  $Q$ , and the cosmological constant only. From the tables and figures we find the following properties for the quasinormal frequencies: a) The magnitude of the imaginary part of the quasinormal mode frequencies decreases as the cosmological constant increases for fixed  $Q$ ,  $kj$ , and  $n$ , but it increases as the charge increases for fixed  $kj$ ,  $n$ . b) The magnitude of the imaginary part decreases as  $kj$  (which relates to the orbital angular momentum) increases for fixed  $n$ ,  $kj$ , and  $Q$ , but it

increases as the overtone number  $n$  increases for fixed  $|q|$ , and  $Q$ . And c) An interesting feature is that the imaginary part is almost linearly related to the real part as cosmological constant changes for fixed charge, and the linearity becomes better as  $|q|$  increases. We also prove exactly that the Dirac quasinormal frequencies of the Reissner-Nordstrom de Sitter black hole (with the same  $|q|$ ). We should note that the orbital angular momentum is different, i.e.,  $l_p$  for particles with potential  $V_1$  and  $l_{ap} = l_p + 1$  for antiparticles with potential  $V_2$ ) are the same for opposite chirality.

#### Acknowledgments

I would like to thank Prof. Ian G. Moss for helpful discussion. This work was supported by the National Natural Science Foundation of China under Grant No. 10275024; and the FANEDD under Grant No. 2003052.

- [1] V. P. Frolov, and I.. D . Novikov, Black hole physics: basic concepts and new developments (Kluwer Academic publishers, 1998).
- [2] S. Chandrasekhar, and S. Detweiler, Proc. R. Soc. Lond. A 344, 441 (1975).
- [3] S. Hod, Phys. Rev. Lett. 81, 4293 (1998).
- [4] O. Dreyer, Phys. Rev. Lett. 90, 081301 (2003).
- [5] C. V. Vishveshwara, Nature, 227, 936 (1970).
- [6] K. D. Kokkotas and B. G. Schmidt, Living Rev. Rel. 2, 2 (1999).
- [7] H. P. Nollert, Class. Quantum Grav. 16, R519 (2000).
- [8] J. Baez, in Matters of gravity. p. 12 ed. J. Pullin, gr-qc/0303027.
- [9] G. Kunstatter, gr-qc/0212014; L. Motl, gr-qc/0212096; A. Corichi, gr-qc/0212126; L. Motl and A. Neitzke, hep-th/03031173; A. M. van den Brink, gr-qc/0303095.
- [10] J. Maldacena, Adv. Theor. Math. Phys. 2, 231 (1998).
- [11] E. Witten, Adv. Theor. Math. Phys. 2, 253 (1998).
- [12] S. Kalyana Ramam and Sathiyapalan, Mod. Phys. Lett. A 14, 2635 (1999).
- [13] J. S. F. Chan and R. B. Mann, Phys. Rev. D 55 7546 (1997).
- [14] D. Birmingham, I. Sachs, and S. N. Solodukhin, Phys. Rev. Lett. 88 151301 (2002).
- [15] V. Cardoso and J. P. S. Lemos, Phys. Rev. D 63 124015 (2001).
- [16] R. A. Konoplya, Phys. Rev. D 66 084007 (2002).
- [17] A. O. Starinets, Phys. Rev. D 66 124013 (2002).
- [18] G. T. Horowitz and V. E. Hubeny, Phys. Rev. D 62 024027 (2000).
- [19] Y. Kurita and M. A. Sakagami, Phys. Rev. D 67 024003 (2003).
- [20] V. Cardoso and J. P. S. Lemos, Phys. Rev. D 64 084017 (2001).
- [21] V. Cardoso, R. Konoplya, and J. P. S. Lemos, gr-qc/0305037.
- [22] R. A. Konoplya, Phys. Rev. D 66 044009 (2002).
- [23] S. Perlmutter, et al, Astrophys. J 483 565 (1997).
- [24] R. R. Caldwell, R. Dave, and P. J. Steinhardt, Phys. Rev. Lett. 80 1582 (1998).
- [25] P. M. Garnavich, et al, Astrophys. J 509 74 (1998).
- [26] I. G. Moss and J. P. Norman, Class. Quant. Grav. 19 2323 (2002); F. M. Mellor and I. G. Moss, Phys. Rev. D 41 403 (1990).
- [27] V. Cardoso and J. P. S. Lemos, Phys. Rev. D 67 084020 (2003).
- [28] C. Molina, Phys. Rev. D 68 064007 (2003).
- [29] A. M. van den Brink, Phys. Rev. D 68 047501 (2003).
- [30] V. Suneeta, gr-qc/0303114.
- [31] A. Zhidenko, gr-qc/0307012.
- [32] D. R. Brill and J. A. Wheeler, Rev. Mod. Phys. 29, 465 (1957);
- [33] H. T. Cho, Phys. Rev. D 68 024003 (2003).
- [34] S. Chandrasekhar, The mathematical theory of black holes (Oxford University Press, Oxford, England, 1983).
- [35] E. W. Leaver, Proc. Roy. Soc. Lon. A 402, 285 (1985).
- [36] G. Poshland E. Teller, Z. Phys. 83 143 (1933).
- [37] V. Ferrari and B. Mashhoon, Phys. Rev. Lett. 52, 1361 (1984).
- [38] V. Ferrari and B. Mashhoon, Phys. Rev. D 30, 295 (1984).

TABLE I: Dirac quasinormal mode frequencies for potential  $V_1$ :  $|k| = 1, n = 0$ 

$l$	$Q = 0.0$	$Q = 0.1$	$Q = 0.2$	$Q = 0.3$	$Q = 0.4$	$Q = 0.5$	$Q = 0.6$
= 0.00	0.1890-0.1048i	0.1893-0.1048i	0.1903-0.1049i	0.1921-0.1050i	0.1946-0.1051i	0.1982-0.1052i	0.2029-0.1052i
= 0.02	0.1712-0.0939i	0.1715-0.0940i	0.1727-0.0942i	0.1746-0.0945i	0.1773-0.0949i	0.1812-0.0954i	0.1862-0.0959i
= 0.04	0.1513-0.0821i	0.1517-0.0822i	0.1529-0.0825i	0.1550-0.0831i	0.1581-0.0838i	0.1624-0.0847i	0.1680-0.0858i
= 0.06	0.1283-0.0688i	0.1287-0.0689i	0.1302-0.0695i	0.1327-0.0703i	0.1362-0.0715i	0.1411-0.0729i	0.1474-0.0746i
= 0.08	0.1001-0.0529i	0.1007-0.0532i	0.1025-0.0539i	0.1056-0.0552i	0.1100-0.0570i	0.1159-0.0593i	0.1235-0.0619i
= 0.09	0.0824-0.0432i	0.0831-0.0436i	0.0853-0.0446i	0.0890-0.0462i	0.0942-0.0485i	0.1010-0.0513i	0.1096-0.0547i
= 0.10	0.0597-0.0311i	0.0607-0.0315i	0.0637-0.0330i	0.0685-0.0353i	0.0751-0.0384i	0.0834-0.0421i	0.0936-0.0464i
= 0.11	0.0189-0.0097i	0.0218-0.0112i	0.0290-0.0148i	0.0384-0.0196i	0.0491-0.0249i	0.0610-0.0306i	0.0743-0.0366i

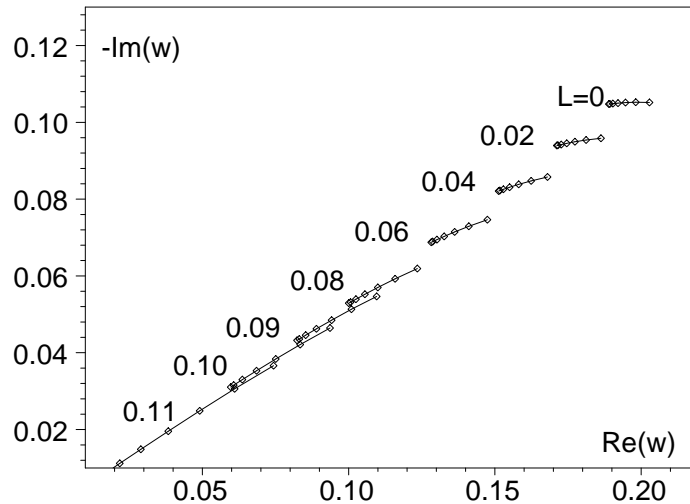
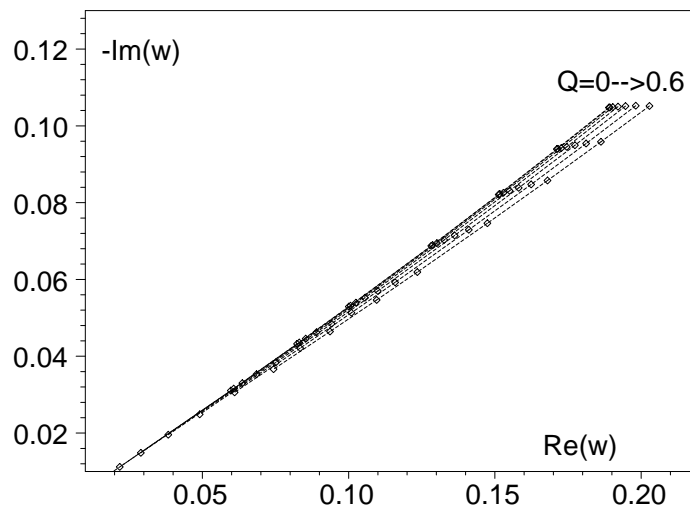
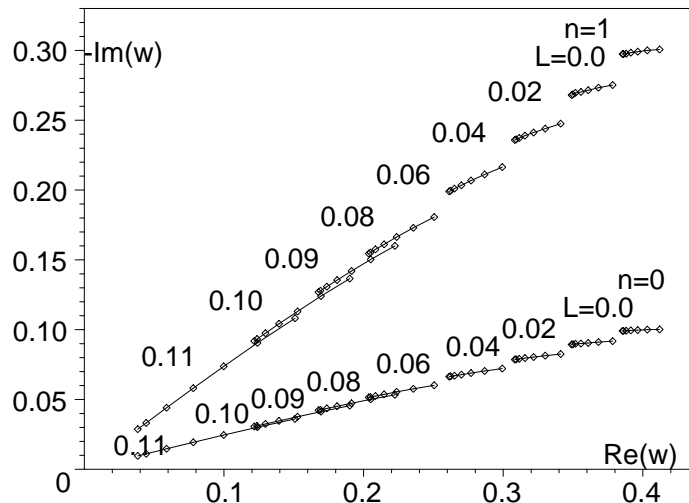
FIG. 1: Dirac quasinormal mode frequencies for the potential  $V_1$ :  $|k| = 1, n = 0$ . The lines are drawn for  $l = L = 0; 0.02; 0.04; 0.06; 0.08; 0.09; 0.10; 0.11$ .FIG. 2: Dirac quasinormal mode frequencies for the potential  $V_1$ :  $|k| = 1, n = 0$ . The lines are drawn for  $Q = 0; 0.1; 0.2; 0.3; 0.4; 0.5; 0.6$ .

TABLE II: Dirac quasinormal mode frequencies for potential  $V_1: |k| = 2, n = 0$ 

!	$Q = 0.0$	$Q = 0.1$	$Q = 0.2$	$Q = 0.3$	$Q = 0.4$	$Q = 0.5$	$Q = 0.6$
= 0.00	0.3855-0.0991i	0.3861-0.0991i	0.3881-0.0993i	0.3915-0.0995i	0.3964-0.0997i	0.4031-0.1000i	0.4121-0.1003i
= 0.02	0.3490-0.0894i	0.3497-0.0894i	0.3519-0.0897i	0.3556-0.0900i	0.3610-0.0905i	0.3684-0.0911i	0.3783-0.0917i
= 0.04	0.3083-0.0786i	0.3091-0.0787i	0.3115-0.0791i	0.3157-0.0796i	0.3218-0.0804i	0.3301-0.0814i	0.3411-0.0825i
= 0.06	0.2612-0.0663i	0.2622-0.0665i	0.2651-0.0670i	0.2700-0.0678i	0.2771-0.0690i	0.2867-0.0704i	0.2993-0.0722i
= 0.08	0.2037-0.0515i	0.2049-0.0518i	0.2086-0.0525i	0.2148-0.0537i	0.2237-0.0555i	0.2355-0.0576i	0.2506-0.0603i
= 0.09	0.1677-0.0423i	0.1692-0.0426i	0.1737-0.0436i	0.1811-0.0452i	0.1915-0.0474i	0.2051-0.0501i	0.2224-0.0534i
= 0.10	0.1217-0.0306i	0.1237-0.0311i	0.1297-0.0325i	0.1394-0.0347i	0.1527-0.0377i	0.1695-0.0413i	0.1900-0.0455i
= 0.11	0.0384-0.0096i	0.0444-0.0111i	0.0590-0.0147i	0.0781-0.0194i	0.0999-0.0246i	0.1241-0.0302i	0.1509-0.0361i

TABLE III: Dirac quasinormal mode frequencies for potential  $V_1: |k| = 2, n = 1$ 

!	$Q = 0.0$	$Q = 0.1$	$Q = 0.2$	$Q = 0.3$	$Q = 0.4$	$Q = 0.5$	$Q = 0.6$
= 0.00	0.3855-0.2972i	0.3862-0.2974i	0.3881-0.2978i	0.3915-0.2984i	0.3964-0.2992i	0.4031-0.3001i	0.4121-0.3008i
= 0.02	0.3490-0.2681i	0.3497-0.2683i	0.3519-0.2689i	0.3556-0.2700i	0.3610-0.2715i	0.3684-0.2733i	0.3783-0.2753i
= 0.04	0.3083-0.2358i	0.3091-0.2361i	0.3115-0.2372i	0.3157-0.2388i	0.3218-0.2412i	0.3301-0.2441i	0.3411-0.2475i
= 0.06	0.2612-0.1990i	0.2622-0.1995i	0.2651-0.2010i	0.2700-0.2035i	0.2771-0.2069i	0.2867-0.2113i	0.2993-0.2165i
= 0.08	0.2037-0.1545i	0.2049-0.1552i	0.2086-0.1575i	0.2148-0.1612i	0.2237-0.1664i	0.2355-0.1729i	0.2506-0.1807i
= 0.09	0.1677-0.1269i	0.1692-0.1279i	0.1737-0.1308i	0.1811-0.1356i	0.1915-0.1421i	0.2051-0.1504i	0.2224-0.1601i
= 0.10	0.1217-0.0918i	0.1237-0.0932i	0.1297-0.0974i	0.1394-0.1041i	0.1527-0.1131i	0.1695-0.1240i	0.1900-0.1366i
= 0.11	0.0384-0.0289i	0.0444-0.0334i	0.0590-0.0442i	0.0781-0.0582i	0.0999-0.0738i	0.1241-0.0906i	0.1509-0.1082i

FIG. 3: Dirac quasinormal mode frequencies for the potential  $V_1: |k| = 2$ . The lines are drawn for  $\epsilon = L = 0; 0.02; 0.04; 0.06; 0.08; 0.09; 0.10; 0.11$ .TABLE IV: Dirac quasinormal mode frequencies for potential  $V_1: |k| = 5, n = 0$ 

!	$Q = 0.0$	$Q = 0.1$	$Q = 0.2$	$Q = 0.3$	$Q = 0.4$	$Q = 0.5$	$Q = 0.6$
= 0.00	0.9625-0.0966i	0.9641-0.0967i	0.9690-0.0968i	0.9774-0.0971i	0.9898-0.0974i	1.0067-0.0978i	1.0293-0.0982i
= 0.02	0.8719-0.0874i	0.8734-0.0875i	0.8788-0.0878i	0.8880-0.0882i	0.9016-0.0887i	0.9202-0.0894i	0.9448-0.0901i
= 0.04	0.7700-0.0772i	0.7720-0.0773i	0.7781-0.0777i	0.7885-0.0782i	0.8038-0.0790i	0.8246-0.0800i	0.8520-0.0812i
= 0.06	0.6528-0.0654i	0.6551-0.0656i	0.6623-0.0661i	0.6746-0.0669i	0.6923-0.0680i	0.7163-0.0695i	0.7478-0.0712i
= 0.08	0.5092-0.0510i	0.5123-0.0512i	0.5214-0.0520i	0.5369-0.0532i	0.5591-0.0549i	0.5885-0.0571i	0.6265-0.0596i
= 0.09	0.4195-0.0420i	0.4232-0.0423i	0.4342-0.0433i	0.4527-0.0448i	0.4787-0.0470i	0.5129-0.0497i	0.5559-0.0529i
= 0.10	0.3043-0.0305i	0.3096-0.0309i	0.3243-0.0323i	0.3486-0.0345i	0.3819-0.0375i	0.4239-0.0411i	0.4751-0.0452i
= 0.11	0.0962-0.0096i	0.1112-0.0111i	0.1477-0.0147i	0.1955-0.0194i	0.2500-0.0245i	0.3103-0.0301i	0.3773-0.0359i

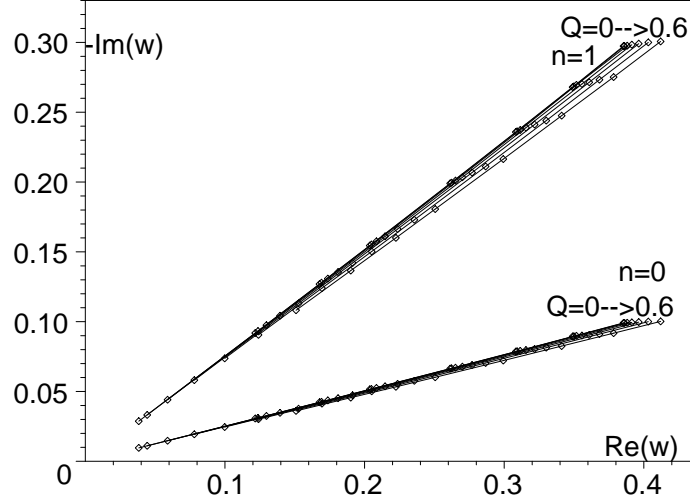


FIG. 4: Dirac quasinormal mode frequencies for the potential  $V_1$ :  $\mathbf{kj} = 2$ . The lines are drawn for  $Q = 0; 0.1; 0.2; 0.3; 0.4; 0.5; 0.6$ .

TABLE V : Dirac quasinormal mode frequencies for potential  $V_1$ :  $\mathbf{kj} = 5, n = 1$

!	$Q = 0.0$	$Q = 0.1$	$Q = 0.2$	$Q = 0.3$	$Q = 0.4$	$Q = 0.5$	$Q = 0.6$
= 0.00	0.9625-0.2899i	0.9641-0.2901i	0.9690-0.2905i	0.9774-0.2913i	0.9898-0.2923i	1.0067-0.2934i	1.0293-0.2946i
= 0.02	0.8716-0.2623i	0.8734-0.2626i	0.8788-0.2633i	0.8880-0.2645i	0.9016-0.2661i	0.9202-0.2681i	0.9448-0.2703i
= 0.04	0.7700-0.2316i	0.7720-0.2319i	0.7781-0.2330i	0.7885-0.2347i	0.8038-0.2371i	0.8246-0.2401i	0.8520-0.2436i
= 0.06	0.6528-0.1962i	0.6551-0.1967i	0.6623-0.1982i	0.6746-0.2006i	0.6923-0.2041i	0.7163-0.2085i	0.7478-0.2137i
= 0.08	0.5092-0.1530i	0.5123-0.1537i	0.5214-0.1559i	0.5369-0.1596i	0.5591-0.1647i	0.5885-0.1712i	0.6265-0.1789i
= 0.09	0.4195-0.1260i	0.4232-0.1269i	0.4342-0.1298i	0.4527-0.1345i	0.4787-0.1410i	0.5129-0.1491i	0.5559-0.1587i
= 0.10	0.3043-0.0913i	0.3094-0.0928i	0.3243-0.0969i	0.3486-0.1036i	0.3819-0.1124i	0.4239-0.1232i	0.4751-0.1356i
= 0.11	0.0962-0.0289i	0.1112-0.0333i	0.1477-0.0441i	0.1955-0.0580i	0.2500-0.0736i	0.3103-0.0902i	0.3773-0.1077i

TABLE VI: Dirac quasinormal mode frequencies for potential  $V_1$ :  $\mathbf{kj} = 5, n = 2$

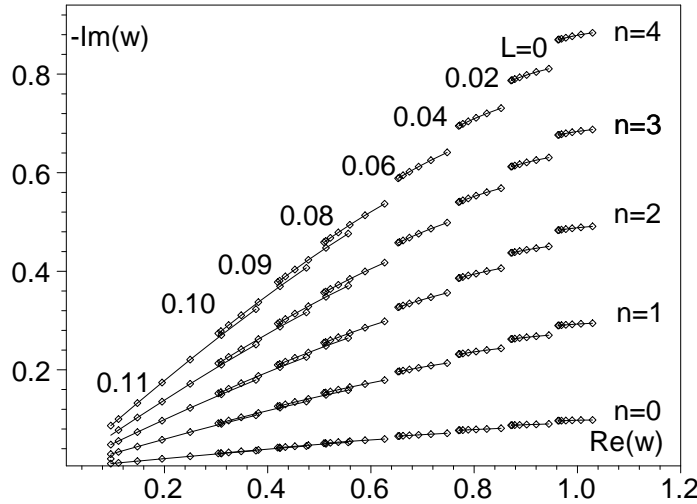
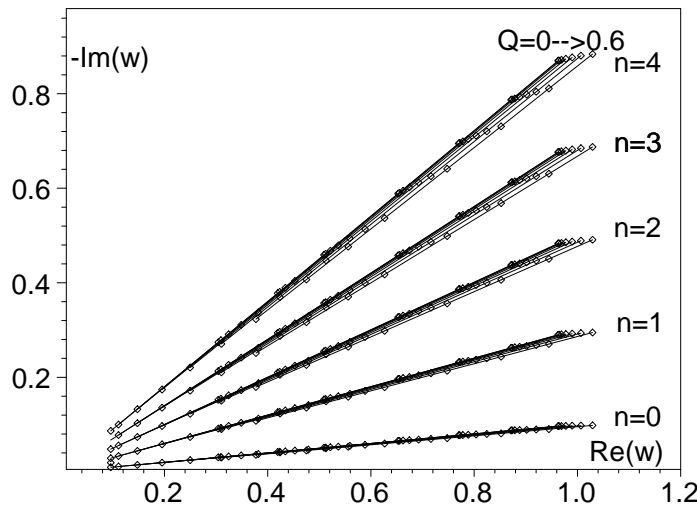
!	$Q = 0.0$	$Q = 0.1$	$Q = 0.2$	$Q = 0.3$	$Q = 0.4$	$Q = 0.5$	$Q = 0.6$
= 0.00	0.9625-0.4832i	0.9641-0.4834i	0.9689-0.4842i	0.9774-0.4855i	0.9898-0.4871i	1.0067-0.4891i	1.0293-0.4910i
= 0.02	0.8716-0.4372i	0.8734-0.4376i	0.8788-0.4388i	0.8880-0.4408i	0.9016-0.4435i	0.9202-0.4468i	0.9448-0.4505i
= 0.04	0.7700-0.3860i	0.7720-0.3866i	0.7781-0.3883i	0.7885-0.3912i	0.8038-0.3951i	0.8246-0.4001i	0.8520-0.4060i
= 0.06	0.6528-0.3270i	0.6551-0.3278i	0.6623-0.3303i	0.6746-0.3344i	0.6923-0.3401i	0.7163-0.3474i	0.7478-0.3562i
= 0.08	0.5092-0.2549i	0.5123-0.2562i	0.5214-0.2599i	0.5369-0.2660i	0.5591-0.2745i	0.5885-0.2853i	0.6265-0.2982i
= 0.09	0.4194-0.2099i	0.4232-0.2115i	0.4342-0.2163i	0.4527-0.2242i	0.4787-0.2350i	0.5129-0.2485i	0.5559-0.2646i
= 0.10	0.3043-0.1522i	0.3094-0.1546i	0.3243-0.1615i	0.3486-0.1726i	0.3819-0.1874i	0.4239-0.2053i	0.4751-0.2260i
= 0.11	0.0962-0.0481i	0.1112-0.0555i	0.1477-0.0736i	0.1955-0.0967i	0.2500-0.1226i	0.3103-0.1503i	0.3773-0.1795i

TABLE VII: Dirac quasinormal mode frequencies for potential  $V_1$ :  $\mathbf{kj} = 5, n = 3$

!	$Q = 0.0$	$Q = 0.1$	$Q = 0.2$	$Q = 0.3$	$Q = 0.4$	$Q = 0.5$	$Q = 0.6$
= 0.00	0.9625-0.6764i	0.9641-0.6768i	0.9689-0.6779i	0.9774-0.6796i	0.9898-0.6820i	1.0067-0.6847i	1.0293-0.6874i
= 0.02	0.8716-0.6121i	0.8734-0.6127i	0.8788-0.6143i	0.8880-0.6171i	0.9016-0.6208i	0.9202-0.6255i	0.9448-0.6307i
= 0.04	0.7700-0.5404i	0.7720-0.5412i	0.7781-0.5436i	0.7885-0.5476i	0.8038-0.5532i	0.8246-0.5602i	0.8520-0.5684i
= 0.06	0.6528-0.4578i	0.6551-0.4590i	0.6623-0.4624i	0.6746-0.4682i	0.6923-0.4762i	0.7163-0.4864i	0.7478-0.4986i
= 0.08	0.5092-0.3569i	0.5123-0.3587i	0.5214-0.3638i	0.5369-0.3724i	0.5591-0.3843i	0.5885-0.3994i	0.6265-0.4175i
= 0.09	0.4195-0.2939i	0.4232-0.2962i	0.4342-0.3029i	0.4527-0.3139i	0.4787-0.3290i	0.5129-0.3479i	0.5559-0.3704i
= 0.10	0.3043-0.2131i	0.3094-0.2164i	0.3243-0.2261i	0.3486-0.2417i	0.3819-0.2623i	0.4239-0.2875i	0.4751-0.3165i
= 0.11	0.0962-0.0674i	0.1112-0.0778i	0.1477-0.1030i	0.1955-0.1354i	0.2500-0.1716i	0.3103-0.2104i	0.3773-0.2513i

TABLE V III: Dirac quasinormal mode frequencies for potential  $V_1: |k|j = 5, n = 4$ 

!	$Q = 0.0$	$Q = 0.1$	$Q = 0.2$	$Q = 0.3$	$Q = 0.4$	$Q = 0.5$	$Q = 0.6$
= 0:00	0.9625-0.8697i	0.9641-0.8702i	0.9689-0.8716i	0.9774-0.8738i	0.9898-0.8768i	1.0067-0.8803i	1.0293-0.8838i
= 0:02	0.8716-0.7870i	0.8734-0.7877i	0.8788-0.7899i	0.8880-0.7934i	0.9016-0.7982i	0.9202-0.8042i	0.9448-0.8108i
= 0:04	0.7700-0.6948i	0.7720-0.6958i	0.7781-0.6989i	0.7885-0.7041i	0.8038-0.7112i	0.8246-0.7203i	0.8520-0.7308i
= 0:06	0.6528-0.5886i	0.6551-0.5901i	0.6623-0.5945i	0.6746-0.6019i	0.6923-0.6122i	0.7163-0.6254i	0.7478-0.6411i
= 0:08	0.5092-0.4589i	0.5123-0.4611i	0.5214-0.4678i	0.5369-0.4788i	0.5591-0.4941i	0.5885-0.5135i	0.6265-0.5368i
= 0:09	0.4195-0.3779i	0.4232-0.3808i	0.4342-0.3894i	0.4527-0.4035i	0.4787-0.4230i	0.5129-0.4473i	0.5559-0.4762i
= 0:10	0.3043-0.2740i	0.3094-0.2783i	0.3243-0.2907i	0.3486-0.3107i	0.3819-0.3373i	0.4239-0.3696i	0.4751-0.4069i
= 0:11	0.0962-0.0866i	0.1112-0.1000i	0.1477-0.1324i	0.1955-0.1741i	0.2500-0.2207i	0.3103-0.2705i	0.3773-0.3230i

FIG. 5: Dirac quasinormal mode frequencies for the potential  $V_1: |k|j = 5$ . The lines are drawn for  $L = 0; 0.02; 0.04; 0.06; 0.08; 0.09; 0.10; 0.11$ .FIG. 6: Dirac quasinormal mode frequencies for the potential  $V_1: |k|j = 5$ . The lines are drawn for  $Q = 0; 0.1; 0.2; 0.3; 0.4; 0.5; 0.6$ .